The content of this manuscript is identical to:

T. Schwarz-Selinger, A. Von Keudell, and W. Jacob.

„Plasma chemical vapor deposition of hydrocarbon films: The influence of hydrocarbon source gas on the film properties“. Journal of Applied Physics 86 (7) (1999): 3988–96. https://doi.org/10.1063/1.371318

Plasma chemical vapor deposition of hydrocarbon films: the influence of hydrocarbon source gas on the film properties

T. Schwarz-Selinger, A. von Keudell, and W. Jacob

Max-Planck-Institut für Plasmaphysik, EURATOM Association

Boltzmannstr. 2, 85748 Garching, Germany

final version, 20. June 1999

Abstract

Hydrocarbon films were prepared by electron cyclotron resonance (ECR) plasma deposition from different hydrocarbon source gases at varying ion energies. The source gases used were the saturated hydrocarbons CH_4, C_2H_6, C_3H_8, C_4H_{10} (n- and iso-) and the unsaturated hydrocarbons C_2H_4 and C_2H_2 as well as mixtures of these gases with hydrogen. Film deposition was analyzed in situ by real-time ellipsometry, and the resulting films ex situ by ion-beam analysis. On the basis of the large range of deposition parameters investigated, the correlation between hydrocarbon source gas, deposition parameters, and film properties was determined. The film properties are found to be influenced over a wide range not only by the energy of the impinging ions, but also by the choice of source gas. This is in contrast to a widely accepted study where no dependence of the film properties on the source gas was observed, this being ascribed to a ‘lost-memory effect’. A strong correlation was found between the hydrogen content of the films and the film properties. This strong correlation is explained on the basis of the random-covalent-network model.

PACS: 81.15.Gh, 68.55.Nq, 78.20.Ci, 52.75.Rx

I. Introduction

Amorphous hydrogenated carbon (a-C:H) films have attracted much interest since they were first mentioned in 1971 [1], because they combine a number of outstanding properties such as high chemical resistance, mechanical hardness, and transparency in the IR. These properties are attractive for a wide range of applications [2] such as protective coatings for optical components, hard coatings for abrasive tools, and biomedical coatings [3,4]. Besides sputtering techniques and ion-beam deposition, a-C:H layers are most often prepared by plasma chemical vapor deposition (PCVD) from hydrocarbon source gases. In these plasmas, the hydrocarbon molecules are dissociated and ionized and the radicals as well as the ions impinging on the substrates lead to the growth of the films. The basic growth mechanisms, however, are still not well understood [5]. It is, for example, not yet clear whether the total growth rate is mainly determined by incorporation of ions [6] or radicals [7] or by synergistic effects among these [5,8,9].

Recent measurements of the particle fluxes emanating from a methane electron cyclotron resonance (ECR) plasma showed that the ion and radical fluxes alone are each able to account quantitatively for the measured deposition rates [10]. Moreover, it was shown that a large variety of species contribute to the particle flux from a methane discharge, due to polymerization in the discharge caused by ion-molecule reactions [5,11,12,13]. This complexity of the particle fluxes has hitherto prevented a complete description of the growth mechanisms. The generally accepted main features of the deposition process are that the film properties depend mainly on the kinetic energy of the ions [5,6,13,14,15], whereas the deposition rate can be significantly influenced by the feed gas [13,14,16,17,18,19,20]. However, a unambiguous correlation between the source gas used and the film properties has not yet been found.

On the one hand, Wild et al. [13,14] postulated that the film properties are rather independent of the hydrocarbon source gas if the films are deposited at sufficiently high ion energies. They further stated that at low ion energies structural units of the precursor are found in the film structure, but at high ion energies complete dissociation and ion-induced mixing of the incoming species lead to a given film structure independent of the hydrocarbon source gas. They coined the name ‘lost-memory effect’ for the fact that at high ion energies the properties of hard a-C:H films do not depend on the hydrocarbon gas used for deposition, because the structural and chemical properties of the precursor molecules get completely lost in the deposition process. However, this widely accepted conclusion was derived from a rough comparison of the infrared spectra of films deposited by n-hexane and benzene plasmas, and of the refractive indices of layers deposited from n- and cyclo-hexane, benzene, and methane. Although their results show a difference in the refractive indices, they considered this insignificant due to the uncertainties in determining the refractive index from optical absorption spectra and because this variation is small compared with the variation that can be achieved by varying the bias voltage. For deposition they used capacitively-coupled RF discharges, applying a wide variety of source gases. High and low ion energies correspond in their studies to deposition at a DC self-bias voltage of 400 and 100 V, respectively, at a process pressure of 3 Pa. In addition, it has to be kept in mind that in an RF discharge the ion energy distribution is very broad, ranging from almost 0 to slightly above the applied DC self-bias voltage [13].

On the other hand, Andry et al. [18] found that, for example, the use of benzene as source gas leads also at high ion energies to film properties different from those deposited from saturated hydrocarbons such as methane and ethane. Grill et al. [19] deposited films with higher refractive index from acetylene than from cyclo-hexane, confirming the influence of the precursor gas, and Uk Oh et al. [20] advocated considering the precursor gas as an experimental parameter to control the properties of deposited films even in ion-beam deposition. Finally, Küppers and co-workers [21] showed for ion-beam-deposited films that the H/C ratio of the films roughly follows the H/C ratio in the hydrocarbon feed gas.

These conclusions were drawn from experiments with very different deposition methods in a limited parameter field, which makes it impossible to find the overall correlation between film properties and source gas. The aim of the present work is, therefore, to investigate the influence of the precursor gas on the film properties for film deposition by PCVD in the very same deposition device on the basis of a large variation in the parameter field. These experiments used seven hydrocarbon source gases (CH_4, C_2H_6, C_3H_8, n-C_4H_{10}, iso-C_4H_{10}, C_2H_4, C_2H_2) which differ in hydrogen-to-carbon ratio, carbon chain length, and hybridization of the carbon atoms, and mixtures of these gases with hydrogen. As a further experimental parameter, we varied the ion energy during deposition. The film properties were characterized by real-time in-situ ellipsometry and their composition was derived quantitatively by ion-beam analysis.

II. Experiment

a) Film Preparation

Preparation of the C:H films from the different source gases was done with a remote electron cyclotron resonance (ECR) plasma. A magnetic field was applied to obtain the resonant field of 87.5 mT. The absorbed microwave power in the plasma was measured by directional couplers, yielding an average power density in the plasma volume of about 10 kW m^{-3}. Films with thicknesses of up to 300 nm were deposited on single-crystalline silicon substrates mounted on an RF-driven electrode in order to vary the ion energy through the DC self-bias induced by the applied RF power. Details of the setup can be found in [22].

The total pressure during deposition was set at 0.2 Pa. At this low pressure the sheath is considered to be collisional-free so that the measured DC self-bias voltage V_b plus the floating potential (about -10 to 15 V, see ref. [5], Fig. 6 and sect. 6.2) corresponds directly to the ion energy. This DC self-bias was adjusted by the RF power additionally applied and ranged from floating potential up to -250 V.

To obtain decoupling of the film deposition and the plasma as source for the ions and radicals, a metallic cage was used to confine the plasma. Through an aperture in the cage (35 mm in diameter) a plasma beam is extracted for the deposition of the C:H layers. In this set-up, changes of the DC self-bias do not influence the production of ions and radicals in the bulk plasma. This decoupling of ion energy and ion flux cannot be achieved by means of conventional RF discharges.

The gas flow was measured by flow controllers and ranged from 15 sccm (CH_4) to 35 sccm (C_2H_2). In general, the pressure after ignition of the discharge is lower than that before ignition. The pressure drop depends on the gas used and is largest for C_2H_2. The experiments were performed at constant pumping speed, and so the gas

flow had to be adjusted accordingly to maintain the same operating pressure for the different precursor gases. This experimental procedure leads to identical residence times for stable species in the different plasmas. It should be noted that many other studies published were conducted at constant gas flow with varying pumping speed to adjust the operating pressure. This yields variable residence times for different gas compositions.

The surfaces were decontaminated by treating the silicon substrates with an oxygen plasma at floating potential for ten minutes prior to deposition. Because of the compressive stress for films deposited with an additional self-bias, it was found to be additionally necessary to remove the SiO_2 surface layer to achieve good adhesion. The substrates were, therefore, exposed in these cases to a hydrogen plasma at a DC self-bias of -200 V for 15 minutes, which completely removes the oxide. The removal of the oxide was checked by in-situ real-time ellipsometry. Longer treatment times result in the build-up of a hydrogenated silicon surface which is also made visible by in-situ ellipsometry.

The deposition was performed without additional external heating and the substrate temperature was measured by a thermocouple in the electrode. For measurement of the data presented in Figs. 1 to 4 the substrates were bonded to the electrode by means of a colloidal carbon glue. This warrants excellent thermal contact between the sample and electrode. The electrode temperature measured by the thermocouple was regularly compared with the substrate surface temperature by in-situ real-time ellipsometry as described in [23]. In general, excellent agreement between the two values was achieved. The deposited layers were removed after each deposition run by means of an oxygen discharge and the next experiment was performed with the same substrate, so that a single silicon substrate was, in general, used for a whole series of measurements. Due to the impinging ion flux the temperature of the substrate rose during deposition. The actual temperature increased with increasing applied bias voltage. The highest substrate temperature of about 420 K was measured for V_b = -250 V at the end of the deposition cycle. The substrate temperature at floating potential was always below 320 K. In general, the temperature rose quickly in the first 5 minutes to about 70 - 80% of the total temperature increase, followed by a slow continuous increase for the remaining deposition time. Typical total deposition times are 15 to 20 minutes. The maximum surface temperature in the case of bonded substrates was still so low that no temperature-induced structural changes had to be anticipated [24,25]. Samples produced for ex situ analysis were not bonded to the electrode, since they had to be removed after each deposition run. In that case, the surface temperature was higher than the thermocouple temperature. The precise temperature values are not known, but it is assumed that for the depositions at V_b = 0 and -30 V this temperature rise is relatively moderate; however, at V_b = -200 V it can be quite substantial. Recent investigations of temperature-induced modifications of a-C:H films have shown that dense and hard a-C:H layers show no notable changes up to about 500 K [24] and significant effects occur above about 600 K [25]. On the other hand, soft polymer-like C:H layers are much more temperature sensitive and measurable changes start to show up above about 350 to 400 K [25]. We measured in our setup for the non-bonded samples under identical plasma conditions slightly higher values for the refractive index. At V_b = 0 and -30 V the refractive indices are about 0.05 higher than for the bonded samples, and at V_b = -200 V about 0.1 higher. The refractive indices for the samples presented in Figs. 5 to 7 are, therefore, slightly higher than those for Figs. 1 to 4. This does not, however, influence our conclusions, since they are not based on quantitative comparisons between these two sets of samples.

b) Thin Film Analysis

A rotating analyzer ellipsometer (RAE) was used to measure the ellipsometric angles Ψ and Δ [26,27,28] during deposition of the films. Details of the ellipsometric setup are presented elsewhere [29]. All the experiments presented in this article were performed at a wavelength of 600 nm.

From the measured ellipsometric angles the complex refractive indices ($n^* = n - ik$) of the films were determined by means of an optical model as described elsewhere [22,29]. For the in-situ investigations we always deposited films with a thickness leading to at least a full revolution in the Ψ-Δ plane (Δ changes by more than 360°) to achieve high sensitivity for n as well as k. These thicknesses correspond to about 130 nm for dense and hard layers (n = 2.4) and 240 nm for soft polymer-like layers (n = 1.57). Best agreement between the data and the optical model was found by assuming uniaxial anisotropy in the deposited films: the complex refractive index was found to be slightly higher in the direction perpendicular to than in that parallel to the film surface. This might be due to the compression of the carbon network during deposition because of the directional ion flux. The absolute accuracy of the agreement of the optical model with the ellipsometric data depends on the density of the films. For soft, polymer-like films the uncertainty is lower than $1*10^{-2}$ and $5*10^{-4}$ for the real and the imaginary part of the refractive index, respectively. For dense hydrocarbon films the uncertainties are higher and the values are $2*10^{-2}$ and $1*10^{-2}$, respectively.

The composition of the films was analyzed quantitatively by ion-beam analysis. Proton-enhanced cross-section scattering (PES) was used to determine the areal density of carbon in the films, and elastic recoil detection (ERD) was applied to measure the areal density of hydrogen atoms as described elsewhere [30,31]. New cross-section data from Amerikas et al [32] for PES and from Baglin et al. [33] for ERD were applied for the analysis.

The film thickness was determined from the in-situ real-time ellipsometric measurements, but it was also measured ex situ with a commercial profilometer (Tencor alpha-step 200). Excellent agreement within the uncertainty of the profilometer (5 nm) was achieved. This film thickness and the areal densities of hydrogen and carbon were used to calculate the total density of the films. The total inaccuracy for the hydrogen and carbon density is about 10%.

Infrared spectra were measured in transmission for films about 300 nm thick deposited on silicon substrates (two sides polished) by means of a Perkin Elmer 1760X Fourier transform infrared spectrometer. From the transmission spectra the extinction k, the imaginary part of the complex refractive index $n^* = n - ik$, was calculated by applying a formalism described in ref. [34]. This formalism takes into account multiple coherent reflections in the thin film and the Kramers-Kronig relation between the real and imaginary parts of the refractive index.

III. Results

In Fig.1 the parallel component of the real part of the index of refraction n_p as measured by real-time in-situ ellipsometry of the films prepared from three different hydrocarbon gases is shown as a function of the applied DC self-bias voltage V_b. As expected from the literature [5,6,13-16], the refractive indices of all films increase as V_b (which corresponds to increasing ion energy). At higher ion energies, above about 100 to 150 eV, the refractive index saturates at a certain value. For each source gas this saturation occurs at a different level, which is in distinct contradiction to the 'lost-memory effect' mentioned above. It should be emphasized that the external deposition parameters such as pressure, absorbed microwave power, and residence time of stable species were the same for the three different preparations, so that the variation of the film properties is caused either by different compositions of the impinging particle fluxes during growth or by the intrinsic properties of the precursor gas. Deposition from acetylene always yields films with the highest refractive index, from ethylene the second highest, and from butane the lowest. All other source gases investigated yield refractive indices between those from ethylene and butane.

Figure 2 shows the dependence of n_p on the precursor gas for three selected bias voltages. As abscissa for this plot we used the H/C ratio in the source gas. However, it has to be kept in mind that this is not a scaleable parameter since the hybridization of the precursor gas changes too. But the figure gives a compact overview of the dependence on the source gas. At all three bias voltages we find a trend of increasing n_p with decreasing H/C ratio, but it also seems that the change of the hybridization of the precursor has a strong influence which is manifested in a substantial increase found for C_2H_4 and C_2H_2.

During deposition, the source gas is dissociated and ionized and the particle flux towards the surface consists of neutral hydrocarbon fragments, a large variety of ions, and atomic hydrogen [5,10-13,35]. In order to investigate the relative contribution of the impinging atomic hydrogen flux, we deposited films with an additional hydrogen fraction in the feed gas. It is assumed that this increases the flux of atomic hydrogen relatively to that of hydrocarbon fragments. The results for the admixture of various fractions of hydrogen to the saturated hydrocarbon gas, n-butane, are depicted in Fig. 3. At DC self-bias voltages below about 50 V this has no significant influence on the refractive index, but at higher ion energies the admixture of hydrogen leads to a substantial decrease of n_p. This decrease of n_p is the stronger the higher the hydrogen admixture is. However, adding more than 50% hydrogen causes only a slight further reduction of n_p, but the deposition rate drops significantly. Similar results have been reported earlier for the admixture of hydrogen to methane (see Fig. 3 in ref. [36]).

In contrast, the addition of hydrogen to the unsaturated hydrocarbon, acetylene, leads to a decrease of the refractive index over the whole range of ion energies. This is shown in Fig. 4, where n_p is plotted versus V_b for several different admixtures of hydrogen to acetylene. The data for acetylene are taken from ref. [36]. Already at floating potential (V_b = 0 V) the admixture of up to 66% hydrogen causes a decrease of n_p from about 1.74 to 1.64 and at V_b = -100 V n_p decreases from about 2.26 to 1.97. It has to be mentioned that the data for n_p previously published by von Keudell and Jacob [36] are about 0.02 lower than the values in Fig. 1. The reason for this difference in not totally clear; it might be due to a slight modification of the experimental setup or to the fact that in the previous experiments a different gas flow

- 20 instead of 35 sccm - was used; but this does not influence our conclusions. The general behavior with respect to the dependence on V_b and hydrogen admixture is, however, in excellent agreement with the data presented in this study. Furthermore, we found that, independently of the hydrocarbon source gas, films with very similar properties are obtained, provided the admixture of hydrogen is sufficiently large. This is also demonstrated in Fig. 4, where, in addition to the data for the hydrogen admixture to acetylene, the data for n-butane from Fig. 1 are repeated. The important fact here is that a crossing of the lines for n-butane and a 1:2 mixture of C_2H_2 and H_2 is found. This means that layers with the same refractive index can be deposited at the same external plasma parameters from different source gases if the right hydrogen admixtures are used. In the specific case shown in Fig. 4 this means that at a DC self-bias voltage of about -70 V films deposited from the 1:2 mixture of C_2H_2 and H_2 yield refractive indices identical to those from pure butane. Since all other source gases investigated yield refractive indices higher than those of n-butane, it is obvious that a large variety of other parameter combinations can be found for which the above statement is also valid.

Table I shows the results for the real and imaginary parts of the refractive index obtained from the optical modeling of the in-situ ellipsometry data of the seven pure hydrocarbon gases for three cases: no additional bias voltage and a self-bias voltage of -30 V and -200 V. It should be borne in mind that these substrates were not bonded to the electrode, so that the deposition temperature was somewhat higher, as discussed in the experimental section, yielding values of n_p slightly higher than presented in Figs. 1 to 4. The dependence of the parallel component of the refractive index, n_p, was shown in greater detail in Fig. 1 for the gases acetylene, ethylene, and butane. The dependence of the other gases not shown in Fig. 1 is very similar to that of butane. As already mentioned, the unsaturated feed gases acetylene and ethylene produce films with the highest values for the real and imaginary part of the refractive index. Although the differences in film properties for films deposited from saturated hydrocarbon source gases (CH_4, C_2H_6, C_3H_8, n- and iso-C_4H_{10}) are very small, the high accuracy of the experimental method allows one to distinguish precisely between films deposited with different source gases. These results are significant and reproducible.

Table I also summarizes the mass density and elemental composition of the films as determined from ion-beam analysis. These data allow conclusions similar to those for the optical properties: Films prepared from saturated hydrocarbon source gases show very little difference in hydrogen content, whereas films prepared with ethylene and acetylene show a significantly lower hydrogen content. For all gases used the hydrogen content decreases with increasing ion energy.

An interesting point is the fact that films prepared with a characteristic value of the refractive index of about 1.75 were not stable. These films peeled from the substrate either during deposition when they exceeded a certain thickness or when they came in contact with air. Such layers were, therefore, not available for the ex-situ measurements and the corresponding data are missing in Tab. I. One explanation for this effect could be the fact that for ion energies of 30 eV or lower (depending on the precursor gas used), which lead to the deposition of films with a refractive index of about 1.75, the resulting compressive stress in these dense films requires a well-adhering interface between the film and substrate. However, at these relatively low ion energies this interface is not yet sufficiently strong. Another possible explanation is the maximum in residual stress observed by Dekempeneer et al. [37] which occurs in this ion energy range.

Real-time in-situ ellipsometry also yields the growth rate, which is a factor of 2 higher for ethylene and 3 for acetylene than for the saturated hydrocarbon gases investigated. However, a more quantitative discussion of this effect would require a detailed knowledge of the impinging particle fluxes, which is beyond the scope of this paper.

The fact that films prepared from saturated hydrocarbon source gases show very similar physical properties, whereas films prepared from ethylene and acetylene differ significantly from them is also manifested in their infrared spectra. This is demonstrated in Fig. 5, where the imaginary part of the refractive index, the extinction k, in the C-H stretching region around 2900 cm^{-1} is shown for all pure source gases investigated for deposition at floating potential. The infrared absorption spectra shown differ in shape and amplitude. Methane, propane, n-, and iso-butane give rise to almost identical absorption bands with a maximum for k of about 0.06. Ethane still has a very similar peak shape, but the maximum is lower (about 0.053). For ethylene the changes of the peak shape are significant and the maximum drops to about 0.046. Finally, the acetylene peak is characterized by a significant change of the peak shape and a drastic drop in amplitude to about 0.03. Also visible is the increasing contribution of sp^2-hybridized CH groups above 3000 cm^{-1} for the acetylene and ethylene absorption peaks. It is noteworthy that the infrared absorption bands for films deposited with additional DC self-bias voltages give rise to more or less structureless broad bands with a shape similar to that of the acetylene band in Fig. 5. The individual amplitudes depend on the applied bias voltage and the source gases used. At V_b = -200 V the maxima are around 0.015 for the saturated hydrocarbon source gases and below 0.01 for acetylene. Details of the infrared analysis will be discussed in a forthcoming publication [38].

Summarizing the dependence of the film structure on the hydrocarbon source gas, we can state that a strong influence of the hybridization of the precursor on the resulting film properties was found and the amount of hydrogen in the plasma is of significant importance for the resulting film properties.

In Fig. 6 the parallel component of the index of refraction n_p as measured by ellipsometry is plotted versus the hydrogen fraction c_H (= H/[H+C]) obtained from ion-beam analysis for all samples listed in Tab. I, which were prepared with different hydrocarbon source gases at varying DC self-bias voltages ranging from floating potential to -200 V. In addition, one data point from a 1:2 mixture of C_2H_2 with hydrogen at V_b = 0 V is shown. The data are also summarized in Tab.1. Despite this wide range of deposition parameters the resulting film properties are located in a rather narrow band such that a particular H/(H+C) ratio of samples deposited with different deposition parameters is uniquely correlated to a particular index of refraction. A correlation similar to that for n_p is found for the film density (Fig. 7). Due to the larger uncertainty in determining the density from ion-beam analysis (uncertainty about 10%), the error bars and the scatter of the data are substantially higher than for the refractive index. A comparison of Figs. 6 and 7 implies that, as anticipated from the Clausius-Mossotti relation, the refractive index and the density of the layers are also closely correlated.

IV. Discussion

The experimental results presented in Figs. 1 to 5 and Tab. I clearly prove that the choice of the precursor gas composition has a distinct influence on the optical properties of plasma-deposited hydrocarbon films. This influence is apparent not only at low ion energies as suggested by Wild et al. [13,14], but also at high ion energies. This result is in clear contradiction to the 'lost-memory effect' postulated by Wild et al. [13,14], but is in good agreement with a number of other studies which also found a dependence of the film properties on the precursor gas [18-21]. This obvious discrepancy between our result and the findings of Wild et al. might have two reasons: First, Wild et al. used a rather insensitive method to determine the refractive index - they determined n from the interference pattern in optical absorption spectra - and considered their own measured differences of about 0.09 for n to be insignificant. But, the relatively large difference of about 0.2 at high ion energies (Fig. 1) should be visible by this technique. Second, they used a capacitively-coupled RF discharge to deposit the films. However, RF discharges give rise to very broad ion energy distributions ranging from 0 V to values slightly above the generated DC self-bias voltage [13], so that this broad ion energy distribution might smear out all precursor-gas-related effects. In contrast, we used an ECR discharge with a very small intrinsic width of the ion energy distribution of about 2 eV for the present experimental conditions [5], which will only be moderately modified by the RF biasing; and the high accuracy of ellipsometry allows one to distinguish the optical properties with high precision.

On the basis of the results presented above, the 'lost-memory effect' has to be reinterpreted as illustrated in Fig. 1: On the one hand, using different hydrocarbon source gases and comparable deposition parameters will produce different film properties; this is indicated by the vertical arrows in Fig. 1, labeled 'different films'. On the other hand, identical film properties can be produced from a variety of source gases by changing, for example, the ion energy; this is indicated by the horizontal arrows in Fig. 1, labeled 'similar films'. Knowledge of the H/(H+C) ratio or the refractive index will therefore not allow the hydrocarbon source gas used for deposition to be deduced. For example, for C_2H_2 at floating potential the resulting film properties are identical to CH_4 and C_3H_8 at -30 V self-bias (see Tab.1) and films deposited from C_2H_2 at -30 V are very similar to those from C_4H_{10} at -100 V (see Fig. 1). The addition of hydrogen to the source gas provides a further experimental parameter to produce films with similar properties from a variety of source gas mixtures at different deposition conditions. For example, ethylene at -30 V yields the same refractive index as the mixture of 25% butane with 75% hydrogen for bias voltages above -100 V (see Figs. 1 and 3), and at about -70 V films deposited from the 1:2 mixture of C_2H_2 and H_2 yield refractive indices identical to those from pure butane (Fig. 4).

Interpretation of the influence of an admixture of hydrogen to the source gas is not straightforward, but it can be rationalized on the basis of a framework for understanding C:H film growth [5] recently suggested by W. Jacob. According to this model, the film structure is determined by the ion irradiation effects, the composition of the impinging particle fluxes, and the nature of the dominant neutral growth precursor. The most important processes of ions are direct incorporation of carbon-carrying ions and displacement of bonded hydrogen, thus creating activated sites ('dangling bonds') to which impinging radicals can bond. The precise nature of these activated sites is not known. They could be weak, stressed, or dangling bonds or any

other kind of intermediate state. For the sake of simplicity, they are called dangling bonds in the following.

Interaction of low-energy ions with C:H films is mainly responsible for the resulting hydrogen content in the film. The displacement and sputtering yield of bonded atoms in a C:H film due to impinging CH_3^+ ions were calculated by Möller [39,40] and Jacob [5], using the TRIM.SP computer code [41]. It was shown that the hydrogen release can be well described in three steps: (i) ion-induced displacement of bonded hydrogen in the films, (ii) local recombination of displaced hydrogen to form H_2, and (iii) release of the hydrogen molecules formed. This reaction pathway was also identified by ion-beam analysis [42,43,44]. This hydrogen release controls the resulting H/(H+C) ratio, which is strongly correlated with other film properties such as optical constants, density, etc. [24].

During growth, film formation takes place in a thin surface layer with a thickness determined by the range of the impinging ions (mainly determined by the range of H^+ ions) [5]. This disturbed surface layer ('growth layer') is apparent due to optical constants higher than those of the bulk material and was observed by in-situ real-time ellipsometry [15,36,45]. This growth layer is characterized by a high density of dangling bonds and experiments have shown that the properties of the deposited films are strongly correlated to the density of dangling bonds in this layer [36,45]. A high density of dangling bonds yields layers with high density and refractive index. Consequently, all processes that influence the density of dangling bonds at the surface should also have an influence on the film properties. Neutral carbon-carrying radicals bond to dangling bonds at the surface. They thus increase the deposition rate and contribute to film growth ('ion-radical synergism'), but they also decrease the number of dangling bonds. This depends, however, on the growth precursor. When acetylene, for example, is used instead of methane, the anticipated dominant growth precursor is the ethinyl radical (C_2H). This radical can produce new dangling bonds if the hybridization is changed upon adsorption (from sp^1 to sp^2 or sp^3). The hybridization of the radical growth precursor, therefore, has a considerable influence on the density of dangling bonds and hence on the film properties. This process explains the higher growth rate and the higher refractive indices for acetylene and ethylene compared with saturated hydrocarbons (see Figs. 1 and 4).

Atomic hydrogen reacts with the surface according to the chemical reactions reviewed in refs. 5 and 21. The dominant effect in the context discussed here is the saturation of dangling bonds, which decreases their number at the surface. Furthermore, part of this surface hydrogen is converted to bulk hydrogen during growth. Increasing the atomic hydrogen flux to the surface, therefore, results in deposition of films with higher hydrogen content, lower density, and lower refractive index. The strong correlation between the hydrogen fraction in the plasma and the film properties was clearly seen in the experiments with additional hydrogen in the feed gas (Figs. 3 and 4).

A detailed description of the influence of the atomic hydrogen flux towards the surface is given in ref. 36 and is summarized as follows: The addition of hydrogen to the precursor gas results in a decrease of the density and refractive index of the layers only if the so increased atomic hydrogen flux to the surface can significantly reduce the density of dangling bonds at the surface. At floating potential the number of dangling bonds at the surface is already low because the displacement yield of the ions is low at these low ion energies [5]. An increased hydrogen flux further decreases the density of dangling bonds, but since this density is already quite low, it

has no significant influence on the material properties. However, at high ion energy ion bombardment efficiently produces dangling bonds. Increasing the hydrogen flux in this case causes a substantial decrease of the density of dangling bonds at the surface and, consequently, the density of the deposited film. These two different cases are seen in Figs. 3 and 4, where depositions from pure butane and acetylene and various admixtures of hydrogen are compared. For butane at low DC self-bias voltages (below about -50 eV) the admixture of hydrogen has a negligible influence on the refractive index; at higher DC self-bias it yields, however, films with a significantly reduced refractive index. Using acetylene instead of saturated hydrocarbons greatly reduces the atomic hydrogen flux to the surface is due to the much lower gas phase hydrogen content. In addition, as mentioned above, the growth precursor, the C_2H radical, can produce dangling bonds due to rehybridization. This warrants a high density of dangling bonds and accordingly, a higher density of the material deposited at the same DC self-bias voltage. Adding hydrogen to an acetylene discharge results in a drastic decrease of the refractive index at high DC self-bias and, in contrast to the situation in Fig. 3, it also has a remarkable influence at floating potential, as shown in Fig. 4, because in this case the density of dangling bonds is also relatively high at floating potential [36].

Furthermore, in the experiments reported here it was found that films with very similar properties are obtained independently of the hydrocarbon source gas, provided the admixture of hydrogen is sufficiently large (see Fig. 4 and the respective discussion). In this situation, the film properties are largely determined by the hydrogen-ion-induced effects within the growth layer [5] - mainly displacement of bonded hydrogen leading to a decrease of the hydrogen content - and to a much lesser extent by the reaction of atomic hydrogen at the very surface. This is again a point of view that differs from the explanation of the ‘lost-memory effect’ as suggested by Wild et al. [13,14]. The film structure is to a large extent determined by the interaction of energetic hydrogen ions because they possess the largest penetration depth and the largest yield for displacement of bonded hydrogen in the layers [5]. In view of this, the memory gets lost not only due to fragmentation of molecular ions at the surface - precursor radicals will also efficiently stick to the surface - but also mainly due to bombardment of the surface with energetic hydrogen ions.

Recent measurements on the gas phase composition in a methane ECR discharge by Pecher and Jacob [35] showed that hydrogen accumulates in the discharge at low pumping speed or due to depletion of the source gas. This might be a reason for the large differences in the literature in respect of the influence of the precursor gas on the resulting film structure because in different experimental setups the actual species fluxes might considerably differ although deposition conditions seem to be comparable.

The last point that has to be discussed is the astonishingly high correlation of the film properties as documented in Figs. 6 and 7. In principle, such correlations are no big surprise since they have been implicitly reported in many publications. Koidl, Wild, and co-workers [13,14], for example, showed a strong correlation of various film properties with deposition parameters, but also with each other. Similar trends have been observed by von Keudell et al. [24]. This seems to be general behavior with a-C:H layers. New in the present work, however, is the clear identification of a correlation between physical properties of the layers. This correlation holds not only for variation of one experimental parameter, e.g. the DC self-bias voltage, with otherwise fixed deposition parameters, particularly with the same deposition gas, but

also for wide variation of deposition parameters such as DC self-bias voltage, precursor gas, and hydrogen admixture as demonstrated in this work. It appears that this high correlation is an intrinsic property of the a-C:H system. Simplifying, we can say that the deposition process determines the hydrogen content, and that all other film properties are then in first order determined only by this resulting hydrogen content.

The existing narrow bands in the hydrogen-content / refractive-index and density / refractive index planes, as shown in Figs. 6 and 7, respectively, can be explained on the basis of the fully constrained network (FCN) model proposed by Angus and Jansen [46]. According to this model, an amorphous network can support only a limited number of bond lengths and angle distortions. A compilation of literature data and comparison with the FCN model by Jacob and Möller [47] showed that due to this fact the FCN model more or less defines for a given hydrogen content the sp^3/sp^2 ratio of the films and vice versa. As a consequence of our results, showing the strong correlation between hydrogen content and refractive index (see Fig. 6), density (see Fig. 7), and atom number density (see Tab.1), the FCN model determines for a given hydrogen content not only the atomic fractions of sp^2- and sp^3-bonded carbon, but also the optical constants of the material. Since a large number of publications (e.g. [13,14]) have shown that the film properties just mentioned are also correlated to many other properties such as hardness and band gap, we may speculate that all properties of plasma-deposited a-C:H layers are more or less determined by their hydrogen content.

V. Conclusion

We investigated the material properties of amorphous hydrogenated carbon films deposited by plasma chemical vapor deposition from 7 different saturated and unsaturated hydrocarbon source gases. It was shown that the precursor gas substantially influences the film properties. The unsaturated hydrocarbons acetylene and ethylene lead to films with higher density, lower hydrogen content and higher refractive index than saturated hydrocarbons. This holds for low and high ion energies. This is in contrast to the literature, where a ‘lost memory’ effect predicts the same film properties independently of the hydrocarbon source gas for deposition at high ion energies. However, analysis of our data showed a ‘lost memory effect‘ in a different way: all films can be characterized by their unique correlation between their hydrogen content H/(H+C) and other film properties such as optical constants, density, etc. On the basis of a given film structure, it is therefore not possible to deduce the precursor gas used for the deposition of these films if the deposition parameters are unknown.

Particular emphasis in future investigations should be placed on mass spectrometry to quantify absolutely the composition of the impinging particle flux and on structure-sensitive thin-film spectroscopies, such as infrared spectroscopy, to distinguish even subtle differences in film structure.

Table Captions

Tab. I: Physical properties of hydrocarbon films deposited from seven different source gases at three different DC self-bias voltages. n_p, n_s, and k_p, k_s represent the parallel (index p) and perpendicular (index s) components of the real (n) and imaginary (k) parts of the refractive index as measured by in-situ ellipsometry. The film composition is obtained from ion-beam analysis. The density is calculated from the stoichiometry and the film thickness. $n_{(H+C)}$ represents the total particle number density. Deposition parameters: pressure p = 0.2 Pa adjusted with gas flow at constant pumping speed, absorbed microwave power density P = 10 kW m^{-3}, samples not bonded to the electrode.

a) V_b = floating

source gas	H/C gas	n_p	n_s	k_p	k_s	ρ (g/cm^3)	$n_{(H+C)}$ ($10^{28} m^{-3}$)	H/(C) film	H/(H+C) film
methane	4	1.565	1.580	0.0005	0.0009	1.0	8.5	0.79	0.44
ethane	3	1.615	1.616	0.0010	0.0015	1.1	9.1	0.75	0.43
propane	2.66	1.595	1.6	0.0007	0.0009	1.0	8.5	0.79	0.44
n-butane	2.5	1.59	1.60	0.0007	0.0009	0.9	8.2	0.89	0.47
iso- butane	2.5	1.59	1.60	0.0015	0.002	1.1	8.9	0.92	0.48
ethylene	2	1.72	1.74	0.0018	0.0032	1.1	9.5	0.79	0.44
acetylene	1	1.800	1.805	0.014	0.015	1.4	11.1	0.69	0.41

b) V_b = -30 V

source gas	H/C gas	n_p	n_s	k_p	k_s	ρ (g/cm^3)	$n_{(H+C)}$ ($10^{28} m^{-3}$)	H/(C) film	H/(H+C) film
methane	4	1.807	1.825	0.0165	0.0185	1.5	12.0	0.69	0.41
ethane	3	1.845	1.86	0.02	0.022	1.6	12.8	0.69	0.41
propane	2.66	1.72	1.75	0.006	0.0085	-	-	-	-
n-butane	2.5	1.729	1.74	0.0017	0.0022	-	-	-	-
iso-butane	2.5	1.69	1.71	0.0006	0.0008	-	-	-	-
ethylene	2	1.945	1.96	0.019	0.021	1.7	13.7	0.64	0.39
acetylene	1	2.09	2.1	0.037	0.045	1.8	14.0	0.54	0.35

c) V_b = -200 V

source gas	H/C gas	n_p	n_s	k_p	k_s	ρ (g/cm^3)	$n_{(H+C)}$ ($10^{28} m^{-3}$)	H/(C) film	H/(H+C) film
methane	4	2.1	2.20	0.075	0.10	1.7	12.1	0.43	0.33
ethane	3	2.22	2.29	0.1	0.11	1.9	13.2	0.47	0.32
propane	2.66	2.23	2.23	0.096	0.14	2.2	14.8	0.41	0.29
n-butane	2.5	2.25	2.3	0.086	0.13	2.1	14.6	0.45	0.31
iso-butane	2.5	2.26	2.28	0.085	0.10	1.9	13.2	0.43	0.30
ethylene	2	2.335	2.4	0.1	0.15	2.2	14.8	0.37	0.27
acetylene	1	2.455	2.5	0.13	0.14	2.4	14.6	0.27	0.21

References

1 S. Aisenberg, R. Chabot, J. Appl. Phys. 42, 2953 (1971).

2 J. Robertson, Surf. Coat. Technol. 50, 185 (1992).

3 A.H. Lettington, Phil. Trans. Roy. Soc. Lond. 342, 287 (1993).

4 A. Bubenzer, B. Dischler, G. Brandt, P. Koidl, J. Appl. Phys. 54, 4590 (1983).

5 W. Jacob, Thin Solid Films 326, 1 (1998).

6 A. von Keudell, Mat. Res. Soc. Symp. Proc. Vol. 388, 355 (1995).

7 L.E. Kline, J. Appl. Phys. 65 (1), 70 (1988).

8 N. Mutsukura, S. Inoue, Y. Machi, J. Appl. Phys. 75 (1), 43, (1992).

9 W. Möller, W. Fukarek, K. Lange, A. von Keudell, W. Jacob, Jpn. J. Appl. Phys., 34, 2163 (1995).

10 P. Pecher, W. Jacob, Appl. Phys. Lett. 73, 31 (1998).

11 W. Jacob, P. Pecher, in Proceedings of 'Frontiers in Low Temperature Plasma Diagnostics II', edited by H.F. Doebele, W.G. Graham, G. Hancock, G. Kroesen, J. Perrin, and N. Sadeghi, (APP, Bochum, Germany, 1997)., pp. 155-158.

12 P. Pecher, W. Jacob, to be published.

13 P. Koidl, C. Wild, R. Locher, R.E. Sah in R.E. Clausing, L.L. Horton, J.C. Angus, P. Koidl (Eds.), 'Diamond and Diamond-like Films and Coatings', NATO-ASI Series B: Physics, Vol. 266, Plenum Press, New York, 1991, p. 243.

14 C. Wild, P. Koidl, J. Wagner, Proc. E-MRS Symp., Strasbourg, Vol. 17, 137 (1987).

15 A. von Keudell, W. Jacob, W. Fukarek, Appl. Phys. Lett. 66 (11), 1322 (1995).

16 L.P. Andersson, S. Berg, H. Norström, R. Orlaison, S. Towta, Thin Solid Films 63, 155 (1979).

17 N. Vedovotto, J.M. Mackowski, R. Pignard, E. Cornil, P Collardelle, Proc. E-MRS Symp., Strasbourg, Vol. 17, 153 (1987).

18 P.S. Andry, P.W. Pastel, W.J. Varhue, J. Mat. Res. 11, 221 (1996).

19 A. Grill, V. Patel, Diamond and Related Materials 4, 62, (1994).

20 J.U. Oh, K.-R. Lee, K.Y. Eun, Thin Solid Films 270, 173, (1995).

21 J. Küppers, Surface Science Reports 22, 251 (1995).

22 B. Landkammer, A. von Keudell, W. Jacob, J. Nucl. Mater. 264, 48 (1999).

23 A. von Keudell, W. Jacob, J. Appl. Phys. 79, 1092 (1996).

24 A. von Keudell, A. Annen, V. Dose, Thin Solid Films 307, 65 (1997).

25 K. Maruyama, W. Jacob, J. Roth, J. Nucl. Mater. 264, 56 (1999).
26 D.E. Aspnes, A.A. Studna, Appl. Opt. 14, 220 (1975).
27 P.S. Hauge, Surf. Sci. 96, 108 (1980).
28 R.W. Collins, Rev. Sci. Instrum. 60, 3212 (1989).
29 W. Fukarek, A. von Keudell, Rev. Sci. Instr. 66, 3545 (1995).
30 D. Boutard, W. Möller, and B.M.U. Scherzer, Phys. Rev. B 38, 2988 (1988).
31 D. Boutard, B.M.U. Scherzer, and W. Möller, J. Appl. Phys. 65, 3833 (1989).
32 R. Amerikas, D.N. Jamieson, and S.P. Dooley, Nucl. Instr. and Meth. B 77, 110 (1993).
33 J.E.E. Baglin, A.J. Kellock, M.A. Crockett, and A.H. Shih, Nucl. Instr. and Meth. B 64, 469 (1992).
34 A. von Keudell, W. Jacob, J. Vac. Sci. Technol. A 15, 402 (1997).
35 P. Pecher, W. Jacob, to be published.
36 A. von Keudell, W. Jacob, J. Appl. Phys. 81, 1531 (1997).
37 E.H.A. Dekempeneer, R. Jacobs, J. Smeets, J. Meneve, Thin Solid Films 217, 56 (1992).
38 T. Schwarz-Selinger, A. von Keudell, W. Jacob, to be published.
39 W. Möller, in R.E. Clausing, L.L. Horton, J.C. Angus, P. Koidl (Eds.), 'Diamond and Diamond-like Films and Coatings', NATO-ASI Series B: Physics, Vol. 266, Plenum Press, New York, 1991, p. 299.
40 W. Möller, Thin Solid Films 228, 319 (1993).
41 W. Eckstein, Computer Simulation of Ion Solid Interaction, Springer Series in Mater. Sci. 10, (Springer, Berlin, 1991).
42 W. Möller and B.M.U. Scherzer, Appl. Phys. Lett. 50, 1870 (1987).
43 W. Möller and B.M.U. Scherzer, J. Appl. Phys. 64, 4860 (1988).
44 W. Möller, Appl. Phys. Lett. 59, 2391 (1991).
45 A. von Keudell, Nucl. Instr. Meth. Phys. Res. B 125, 323 (1997).
46 J.C. Angus, F. Jansen, J. Vac. Sci. Technol. A 6, 1778 (1988).
47 W. Jacob, W. Möller, Appl. Phys. Lett. 63, 1771 (1993).

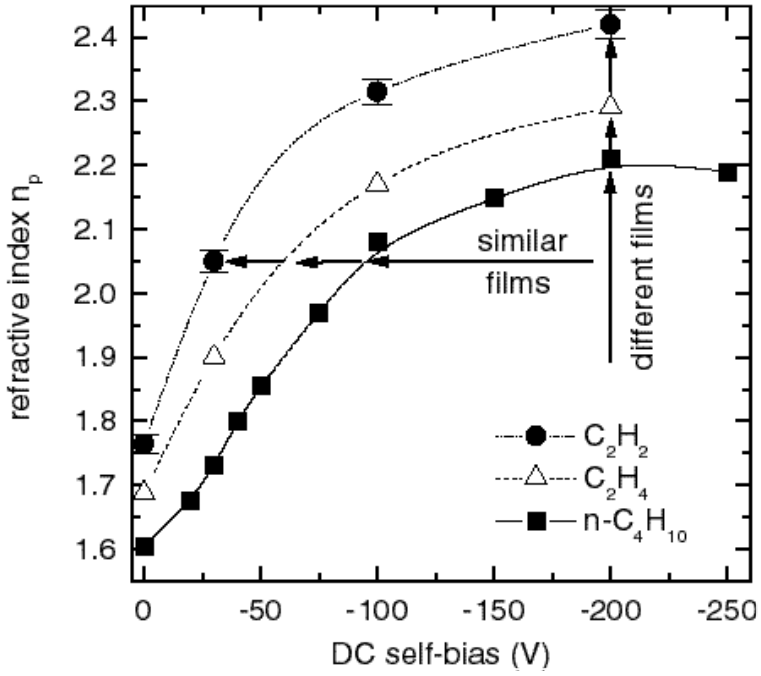

Fig. 1: Parallel component of the real part of the refractive index n_p as a function of the applied DC self-bias voltage for the three precursor gases, acetylene (C_2H_2), ethylene (C_2H_4), and n-butane (n-C_4H_{10}). The lines are only a guide to the eye.

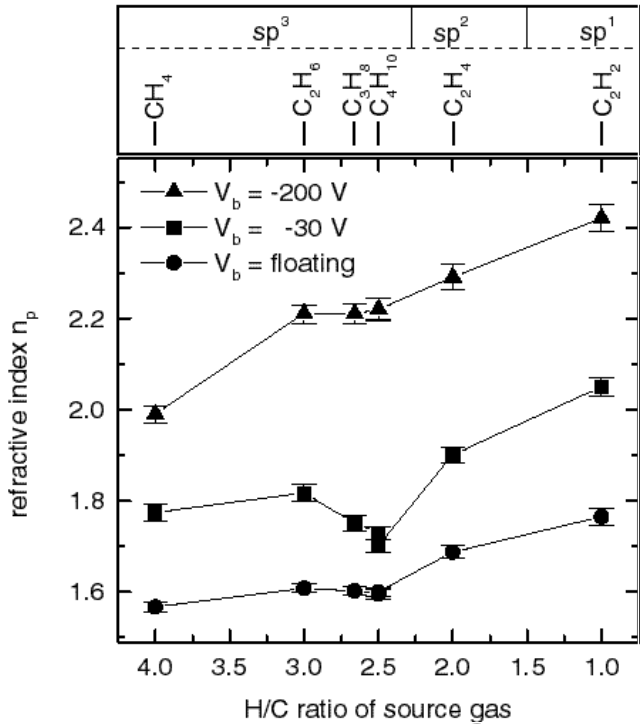

Fig. 2: Parallel component of the real part of the refractive index n_p as a function of the H/C ratio of the precursor gas at three selected values of the applied DC self-bias voltage. It should be kept in mind that this H/C ratio is not a simple scaleable parameter, because the gases also differ in other parameters, e.g. the hybridization. The precursor gases and the respective hybridization of the carbon atoms are also indicated in the figure.

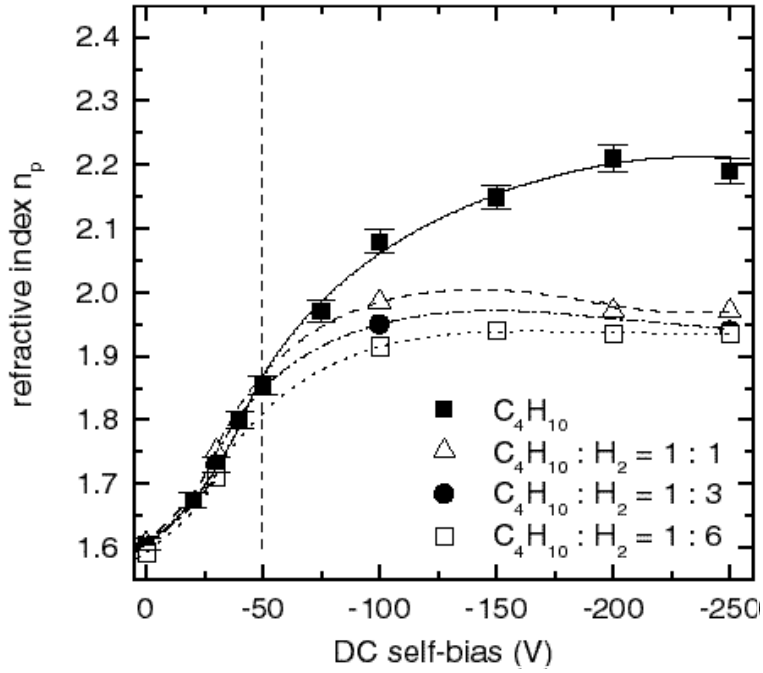

Fig. 3: Parallel component of the real part of the refractive index n_p as a function of the applied DC self-bias voltage for n-butane (n-C_4H_{10}) and gas mixtures of n-butane with various amounts of hydrogen. The lines are only a guide to the eye.

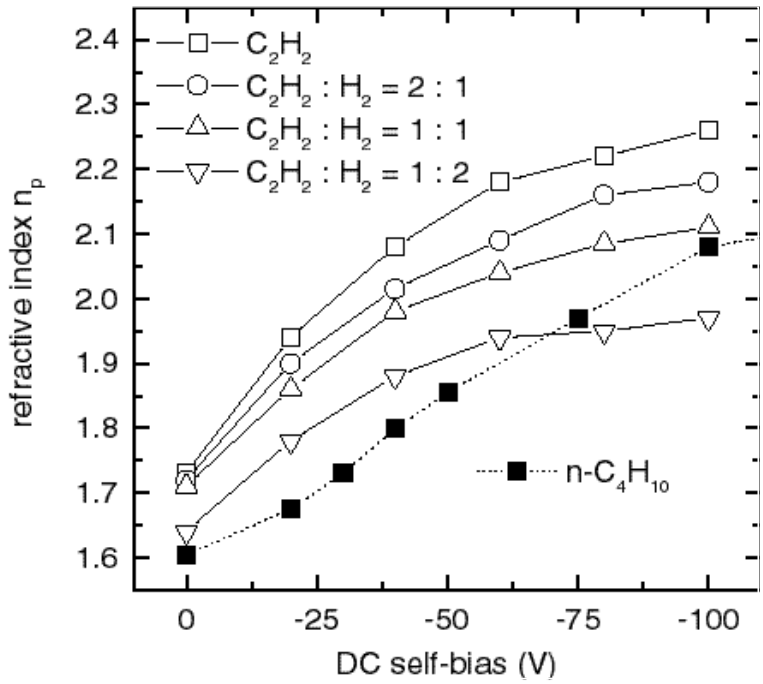

Fig. 4: Parallel component of the real part of the refractive index n_p as a function of the applied DC self-bias voltage for acetylene (C_2H_2) and gas mixtures of acetylene with various amounts of hydrogen (data taken from ref. [36]). Also shown are the data for pure n-butane (n-C_4H_{10}). The lines are only a guide to the eye.

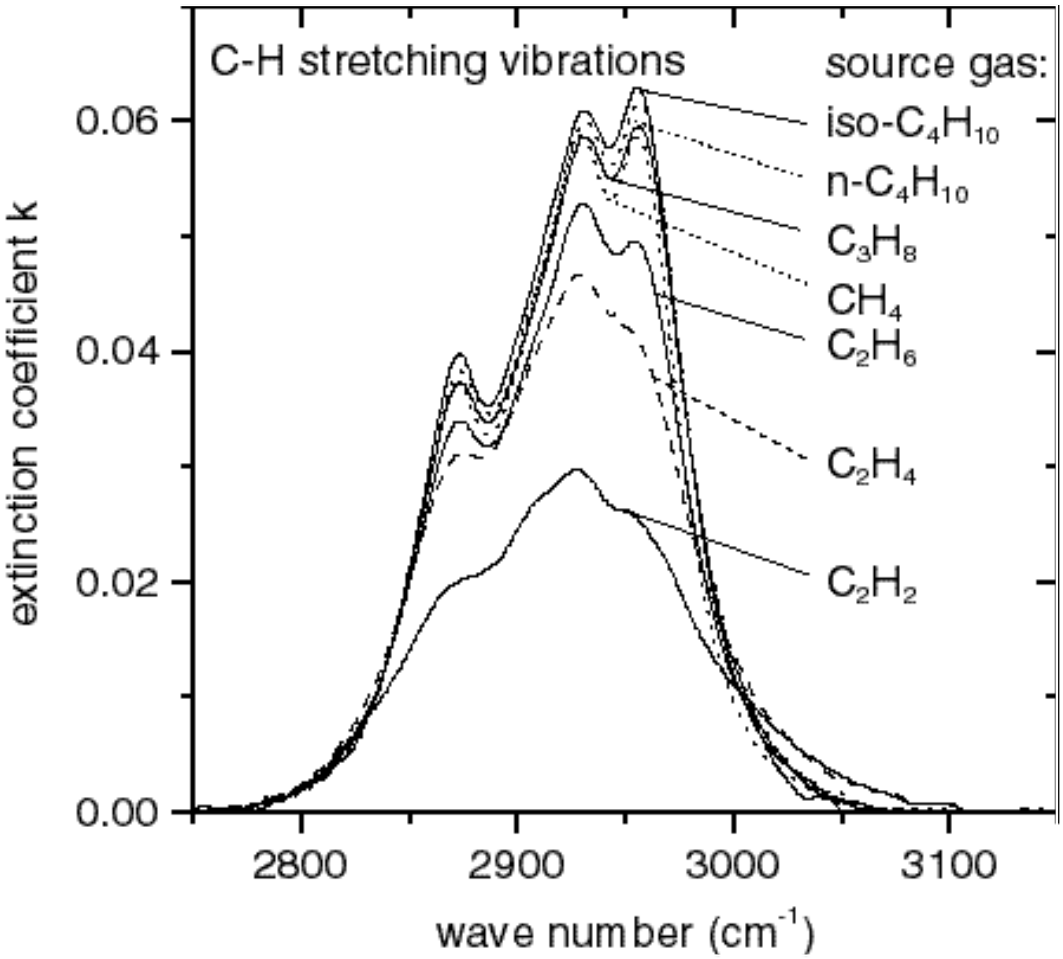

Fig. 5: Extinction coefficient k (imaginary part of the complex refractive index) in the infrared in the range of the C-H stretch vibration around 2900 cm^{-1} for layers deposited at floating potential (V_b = 0) from all gases used. For ethylene and acetylene a slight increase of intensity above 3000 cm^{-1} indicates an increase of sp^2 hybridization in the layers.

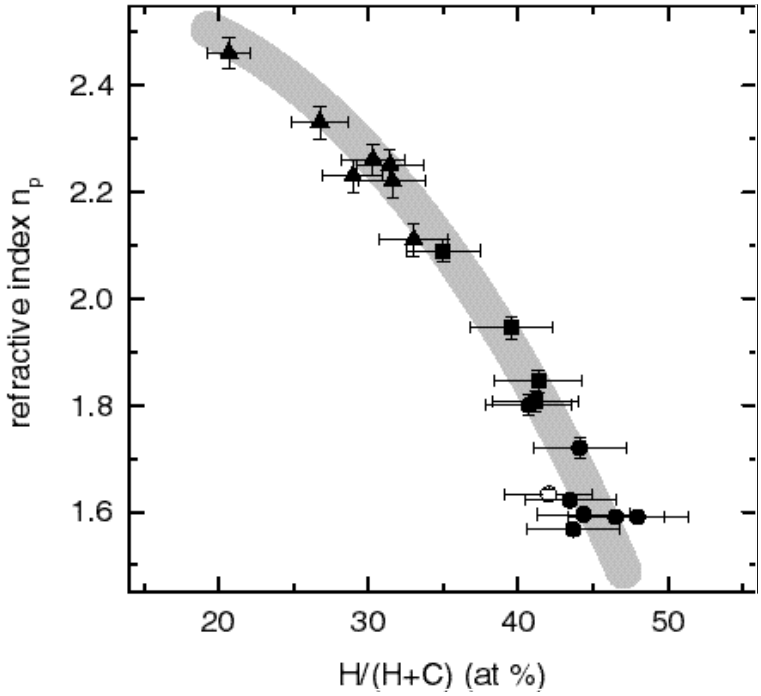

Fig. 6: Parallel component of the real part of the refractive index n_p as a function of the resulting hydrogen content H/(H+C) of the deposited films. Seven different hydrocarbon feed gases and three different DC self-bias voltages were used. The data are also given in Tab. 1. Solid circles correspond to deposition at floating potential (V_b = 0 V), solid squares to V_b = -30 V, and solid triangles to V_b = -200 V. In addition, one data point for a 1:2 mixture of acetylene with hydrogen (deposition at V_b = 0 V) is included (blank circle). The thick gray line is only a guide to the eye. Noteworthy is the strong correlation between these two parameters.

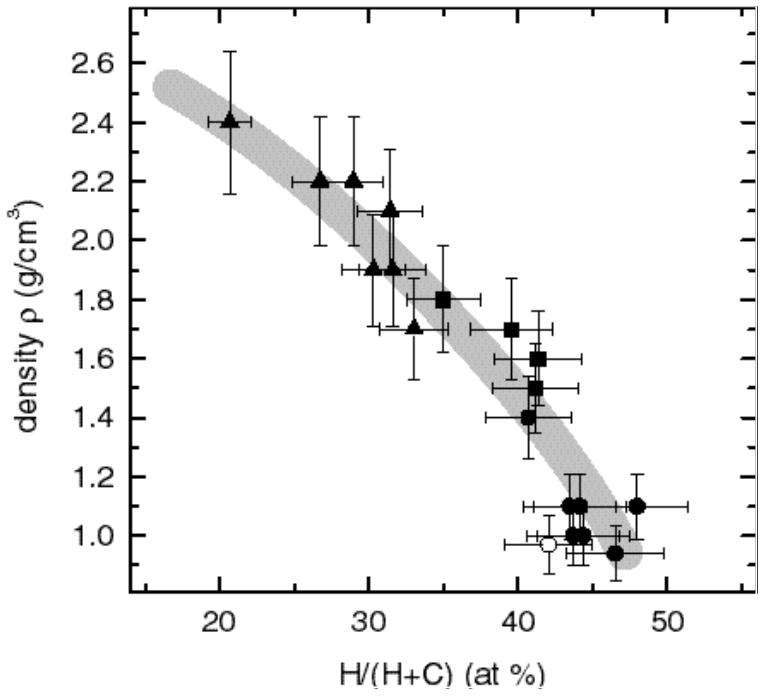

Fig. 7: Density of the deposited layers as a function of the resulting hydrogen content H/(H+C) of the deposited films. For explanation see figure caption of Fig. 6.